



Experimental investigation of polyurea coated aluminum plates under strong hydrodynamic shocks

O. Rijensky^{*}, D. Rittel

Faculty of Mechanical Engineering, Technion- Israel Institute of Technology, 32000, Haifa, Israel

ARTICLE INFO

Keywords:

Polyurea
Plates
Hydrodynamic shocks
Fluid-structure interaction
DIC

ABSTRACT

Polyurea has been used in armor applications for over a decade. Its ability to mitigate shock waves and survive after experiencing large deformations makes it suitable for structural protection purposes. One of the many uses of polyurea coatings is in maritime structures, in which polyurea is not only a mechanical armor but can also serve as chemical protector against corrosion due to its high resistance to environmentally aggressive conditions.

To further implement such applications, one must understand the effect of polyurea coatings on the overall structural response to hydrodynamic shocks.

An experimental investigation of high-pressure shock-loaded polyurea coated aluminum plates is presented. These experiments add to previous experiments that are described in detail in Rijensky and Rittel (2016) [1]. The present experiments reveal the effects of polyurea coating on the fluid structure interaction taking place between shocked water and aluminum plates. This interaction can be the result of numerous scenarios ranging from violent blasts in water to relatively milder loads like wave slamming. Emphasis is put on the selection of the coated side of the aluminum plate, considering those different interactions and their influence on the structure. The presented setup is also an interesting experimental physics case study as the deformation under shock process involves soft materials, fluid-structure interaction and conventional engineering materials deforming all together and affecting one another. Whereas weak shock mitigation was found to favor polyurea on the wet side of the plate, the present work reveals that for strong shocks, polyurea must now be applied on the dry side, thereby revealing a dependence of the optimal placement of the protective layer on the shock intensity.

1. Introduction

With the current global security threats, the demand for cheap and efficient blast protection systems is always on the rise. Offshore structures like oil rigs and tankers are secluded at sea for long periods of time which exposes them to attacks. Combined with the immense costs and stakes, whether economic, political, and environmental, it is not surprising that serious efforts are made to protect these structures. Another concern to maritime structures is the phenomena of wave slamming which threatens the integrity of planning boats and other fast sailing vessels. A most promising lead in designing effective armor is the use of polyurea (referred to as PU) coating. Polyurea was introduced in the 80's as a chemical and abrasion resistant coating. It drew the attention of the defense industry with the work of Amirkhizi et al. [2] who demonstrated its unique shockwave mitigation ability. Since then, many others have studied the characteristics of polyurea with emphasis on its mechanical response. To list a few, Yi et al. [3] investigated the dynamic

properties of polyurea using split Hopkinson pressure bar experiment. Roland et al. [3] studied the behavior of polyurea under tensile loads. Sarva et al. [4] did a similar work for compressive loads. Pathak et al. [5] studied the uniaxial stress response of polyurea to reveal how the glass transition of this polymer affects energy absorption. Mott et al. [6] tried to uncover the thermal effects related to polyurea energy absorption by thermal photography. Knauss et al. [6] confirmed the applicability of the time-temperature superposition principle for polyurea under dynamic loading conditions. Grujicic et al. [7] performed a thorough multi scale investigation, revealing the special micro structure of polyurea and the way it affects its dynamic response.

A few attempts have been made to develop constitutive models for polyurea. The most popular is the one suggested by Amirkhizi [2] following a master curve by Knauss [8]. This model consists of a viscoelastic model with WLF (Williams-Landel-Ferry) [9] time-temperature superposition principle. Hydrostatic pressure dependence is introduced via pressure-time equivalence.

^{*} Corresponding author.

E-mail address: orenrijensky@campus.technion.ac.il (O. Rijensky).

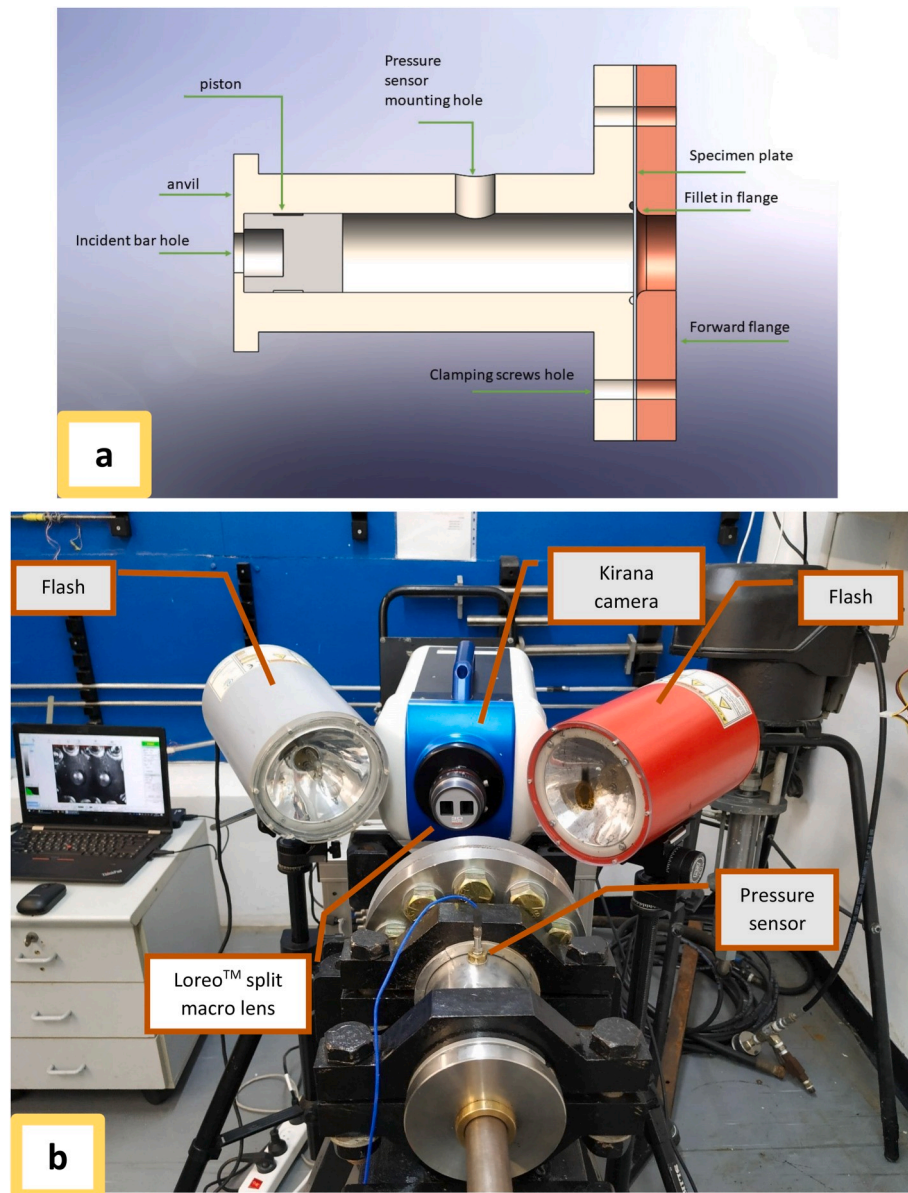


Fig. 1. a. Schematic description of the experimental setup. b. Picture of the setup and its various components used to monitor the impacted diaphragm.

Another model was proposed by Shim & Mohr [10] using two parallel non-linear spring-damper models. Li et al. [11] suggested combining a hyperelastic model for low strain rates with a viscoelastic model for high strain rates. An attempt was made by Bai et al. [12] who used an Ogden model [13] to describe the low strain rate behavior of polyurea, together with a K-BKZ (Bernstein, Kearsley and Zapas) [14] model to describe the viscoelastic nature of the material.

Polyurea has been studied extensively as a coating layer for blast protection [15–20] and for ballistic penetration [21–23]. Some applications that take advantage of the shock mitigation capabilities of the material have also been reported [20,24,25]. The potential of polyurea in maritime applications has also been studied, as it can function for both blast and corrosion protection [26–28].

Optimal placement for polyurea coating in maritime applications was studied both numerically and experimentally by Amini et al. [18, 27] who measured the response of 1 mm thick polyurea coating on DH-36 steel plates to impulsive loading. In this work the loading media were water and soft polyurethane and the pressures reached a maximal value of 800 bar. This work showed the importance of the coating side and provided some initial insights regarding coating thickness. It put the

emphasis on the different types of loads experienced by the polyurea when placed on either side of the specimen plate. When polyurea is placed in contact with the loading medium (“wet polyurea”), it experiences compressive loading which leads to an increase in its bulk modulus, leading to a better impedance matching with the carrying metal plate. On the other hand, when the polyurea is placed on the external side (dry polyurea), it mitigates the relatively lower amplitude stress waves running through it. This work concluded that polyurea coating should not be placed in contact with the loading medium but rather on the other side (subsequently referred to as “dry polyurea”).

Another recent work which should be mentioned here is a recent work by Li et al. [30] who investigated 6061 aluminum plates like the ones studied in this work. They used a flyer plate impacting a piston, generating pressures of the order of 400–700 bar. Their experiment was meant to create a pressure history similar to the characteristic history of an explosion (almost instantaneous pressure peak followed by slower exponential decay). They tested configurations in which the 4-mm thick polyurea coating was placed on the front face (wet polyurea), on the back face (dry polyurea) or sandwiched between the two. Li et al. [30] concluded that coating leads to marginal improvement in terms of shock

mitigation when applied on the front face (wet polyurea), and that the coating should not be split between the two sides.

Another work adding to the controversy about optimal coating placement, is the one of Rijensky and Rittel [1] who conducted a set of experiments aiming to use polyurea as a protective layer against wave slamming in planing boats. This work showed the importance of choosing the coated side (with respect to the load) of the structure for best performance. Their conclusion was that the optimal placement of the polyurea coating layer was at the interface between the fluid and the structure.

The goal of this work is to further examine the importance of the coated side of structural plates under dynamic loading in the specific case of much more violent hydrodynamic shocks. Stated otherwise, we investigate whether the optimal placement of the protective polyurea layer is fixed, or whether it depends on the shock amplitude. Since the emphasis of this work is on polyurea, we chose to use a simple 6061-T6 aluminum alloy plate as the structure to be coated (protected). This material is relatively simple in its mechanical behavior as well as very popular as a structural material for offshore structures. We used a setup capable of creating strong shocks in water, similar to the works presented in Ref. [29,30]. Strains and deformations were measured using a 3D-DIC (digital image correlation) technique [31,32] together with a fast camera system.

2. Experimental setup

2.1. Specimen plates

Circular specimen plates were machined of as-received aluminum 6061-T6 plate, 0.7 mm thick, that were laser-cut to 190 mm diameter with ten 20 mm diameter holes near the plate edge to allow for screw clamping. The plates were coated with Alodine™ primer which enables detachment of the polyurea layer when the aluminum fails, thereby preventing failure in the polyurea due to aluminum whiplashing effect.

Three different sets of specimen plate were tested. Polyurea-coated aluminum plates with the coated side in contact with the water (wet PU), same plates reversed, so that the aluminum was in contact with the water (dry PU), and bare aluminum plates with no coating for reference (no PU). Polyurea coating thickness was about 2.5 mm (varying slightly since the polyurea was spray coated).

The plates were spray painted with a light grey matt spray and then air-brushed with black color to generate a speckle pattern for digital image correlation (DIC) analysis.

The loading setup was comprised of a gas gun accelerating a 25.4 mm diameter C300 maraging steel projectile onto a 1300 mm long maraging steel bar in contact with a 46 mm diameter piston obstructing a 200 mm long maraging steel cylinder. The cylinder is filled with fresh water which gets shocked by the piston. The shock wave travels through the water to hit and deform the investigated specimen (target) plate. Loading was controlled by setting the air pressure in the gas gun pressure vessel. The setup is described schematically in Fig. 1a and shown in Fig. 1b.

2.2. Measurement

Stress waves in the incident bar were recorded using a strain gauge cemented on the bar, and used to estimate the force acting on the piston and pressurizing the water. The strain gauge signal was also used as a camera trigger.

The evolving deformation was captured by a Kirana™ ultra-fast camera equipped with a Loreo™ split lens to capture a 3D image of the specimen plate. A set of 180 consecutive 924×768 images were captured at 50 Kfps, yielding a 0.0036 s long recording. The split lens creates a stereo image of the specimen plates with just one camera. This overcomes the challenge of coordinating two fast cameras to take pictures simultaneously (as shown in Fig. 2). The image is then split into

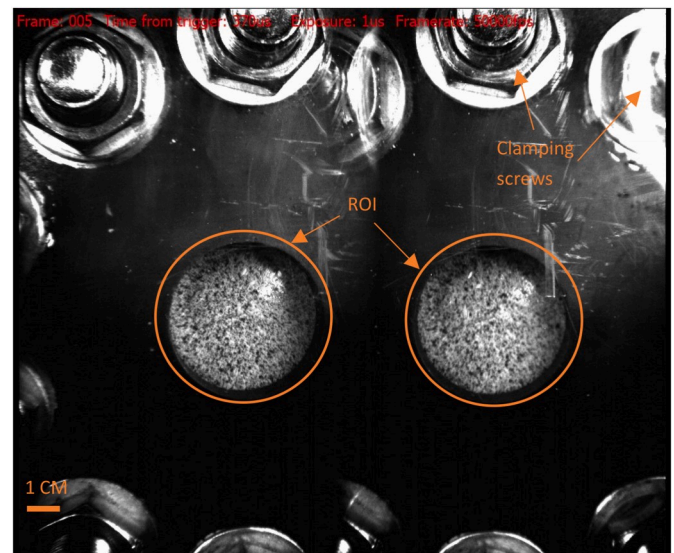


Fig. 2. A specimen plate as taken by the Kirana camera equipped with Loreo split lens, with outlined region of interest.

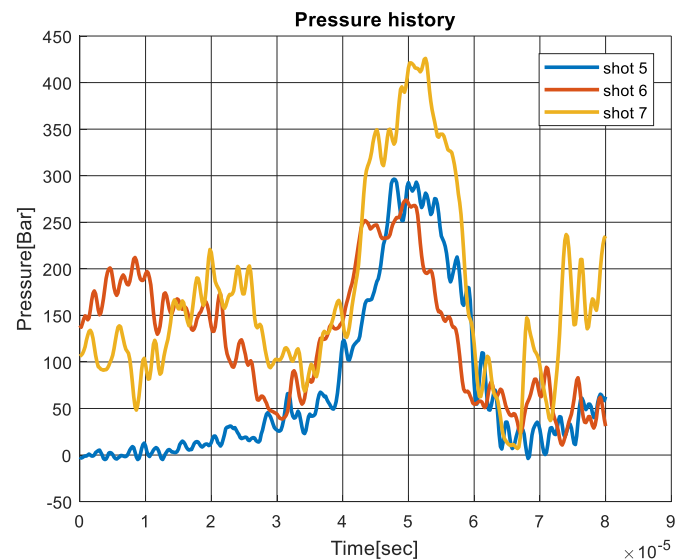


Fig. 3. Pressure histories as recorded in the 3-bar driving pressure experiment. The maximum recorded pressure is of the order of 400 bar.

two images, as if two cameras captured them, like an ordinary stereo photography setup.

The region of interest is photographed with spatial resolution of 5 pixels per millimeter. The error created by the camera calibration process is estimated at 0.1 pixels magnitude. The camera triggered two fast xenon flashlights. The captured images were analyzed using the commercially available Correli STC DIC (digital image correlation) software to obtain the full field of deformation throughout the shock.

Finally, the water pressure was recorded on an oscilloscope using a fast response pressure sensor submerged in the water cylinder. The experimental setup is shown in Fig. 1.

3. Results

Specimen plates were tested under three different gas gun driving pressures: 3 bar, 3.5 bar and 4 bar, respectively.

Table 1

Estimation of impulse transferred to the water. Note the repeatability of the pressure-impulse relationship.

shot	specimen	driving pressure[bar]	impulse[N*sec]
5	dry PU	3	5.48
6	no PU		5.25
7	wet PU		5.28
9	no PU	3.5	6.20E
10	dry PU		N/A
11	wet PU		6.58E
12	wet PU	4	8.61
13	dry PU		8.20

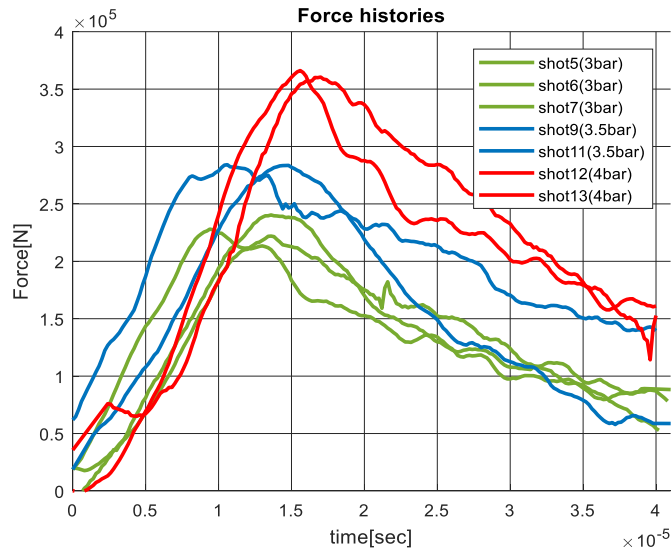


Fig. 4. Recorded load pulses for various pressures. Note the repeatability of the signals, as opposed to the pressure recordings shown in Fig. 3.

3.1. Pressure histories

We first present the pressure histories reached in these experiments. Our previous work showed that coating the side in contact with the water (wet polyurea) is optimal for reducing strains and impeding failure, but that is at odds with the conclusions of Amini et al. [17,28]. With our previous setup, we measured shocks reaching up to 40 bar, which is relatively low. The higher pressure under which Amini’s experiments were conducted may be the reason for the apparent controversy. To solve this issue, an apparatus capable of creating much stronger shock waves than the one used previously was needed, as exemplified in Fig. 3 for the “lower” 3 bar experiments. In fact, the loading pressure in the current experiments was one order of magnitude larger than previously (without accounting for cavitation induced pressure), namely reaching close to 400 bar (Fig. 3). The apparent variability in the recorded signals may be related to the sensor placement inside the pressure cylinder and thus this data will not be used quantitatively to estimate the load exerted on the plates. Rather, to measure the experimental loads, we used the recordings of the strain gauge mounted on the incident bar (summing incident and reflected signals).

3.2. Force histories

Using the strain gauge fitted on the incident bar, strain histories were recorded throughout the shock. By summing the incident and reflected strain waves, one can calculate the force acting on the piston. Time integration yields the impulse transferred through the piston to pressurize the water. Table 1 summarizes the imparted impulses. It can be observed that similar driving pressures result in similar impulses.

Table 2

Central maximal residual deflection of the specimen plates. *± 1 mm.

driving pressure	spec	type	Maximal residual deflection [mm]*
3 bar	5	dry	5
	6	no	7
	7	wet	5
3.5 bar	9	no	10
	10	dry	6
	11	wet	7
4 bar	13	dry	9
	12	wet	breached
	14	no	breached

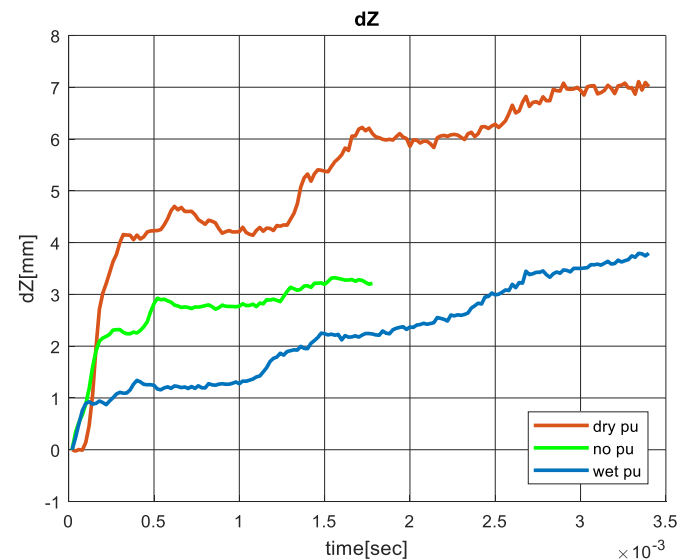


Fig. 5. Center point deflection history under 3 bar driving pressure.

Incident and reflected waves are formed prior to any fluid-structure interaction. With that in mind, we can consider the similar impulses under similar driving pressures as a clear sign of experimental repeatability of the exerted loads, the latter being crucial as we aim to compare different specimen designs under similar conditions.

The recorded force histories are presented in Fig. 4. One can notice the similarity in shape and magnitude of the applied loads for every set of pressures.

3.3. Maximal residual deflection

We now consider the effects of the shock waves on the plates. Firstly, the maximal residual membrane deflections after the shock, are shown in Table 2.

It can be observed that polyurea coating decreases the maximal deflection regardless of the side on which it is applied. One can also notice that under weaker shock waves, wet and dry polyurea perform comparably, but as the pressure rises, the advantage of laying the polyurea on the dry side becomes evident. To gain more insight on the deformation process, we next examine the results obtained throughout the deformation process using fast photography and 3D DIC.

3.4. Center point deflection

Consider first center point deflections of dry polyurea, wet polyurea and no polyurea specimen plates subjected to water pressure history induced by the 3 bar gas gun driving pressure as shown in Fig. 5.

One can note that the wet polyurea specimen delivers the best performance as the center point deflection is smaller and rises in a steadier and more stable rate. The dry polyurea plate reacts most violently to the

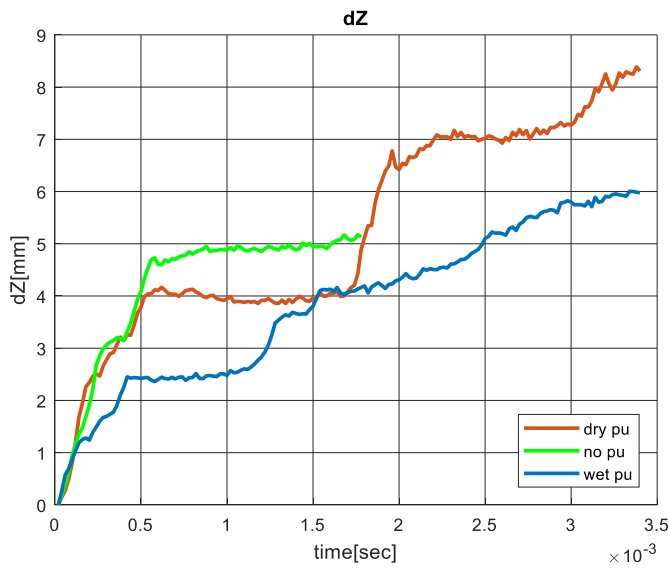


Fig. 6. Center point deflection history under 3.5 bar driving pressure.

shock. The fact that the dry polyurea specimen exhibits the largest central deflections can be the outcome of the polyurea reinforcement. Heavy and rigid structures absorb more momentum than flexible ones during impact, and this can be the reason for the enhanced deformation due to coating on the dry side [30,33]. One may suggest that the reinforcing polyurea causes a reflected wave in the water which leads to water cavitation, as reported in Ref. [1]. As the cavitation bubble bursts, it creates very violent shocks. As this cavitation shock is confined to the center of the plate, this might explain the additional center point deflection in the dry polyurea plate. Another possible explanation to the better performance of the no polyurea plate in comparison with the dry polyurea plate is the no polyurea plate failure at an early stage. Before the plate erupts completely, the speckle paint layer peels and chips and the DIC algorithm “loses” its ability to track the speckles reliably. This leads to a non-reliable measurement of deflections and strains as the paint layer has already separated from the aluminum plate and it moves as a rigid body while the underlying plate still deforms.

The wet polyurea plate deforms more gradually than the dry polyurea plate, as observed in our former work [1]. Applying polyurea to the wet side of a plate has a damping influence on the fluid-structure interaction, which leads to less momentum being transferred from the water to the plate.

The fact that a dry polyurea plate performs more violently than a wet polyurea plate under this test stands in apparent contradiction with the maximal residual deflection results shown in Table 2 (in which both plates performed the same). This contradiction can be settled by remembering that having a polyurea coating on the dry side might dissipate shock waves having propagated through the plate as reported by Ref. [28]. On the other hand, waves that passed through the wet polyurea layer to penetrate the aluminum layer remain “trapped” there and cannot return to the polyurea layer due to impedance mismatch between the layers, resulting in the aluminum layer being exposed to more shock energy and thus increased plastic strain.

Consider next the results obtained for 3.5 bar shot pressure (Fig. 6).

The wet polyurea plate still shows the best performance, namely smaller deflections. The dry polyurea plate deflects less than the non-coated plate (the latter experiencing early failure and early chipping off of the speckle pattern). One can see that the gap in performance between the dry and the wet polyurea plate is narrowing. When considering the maximal residual deflection as summarized in Table 2 we see that the dry polyurea plate performs better than the wet polyurea plate. Again, this might be the outcome of the polyurea layer acting as a “shock absorber” when placed on the dry side in comparison with the

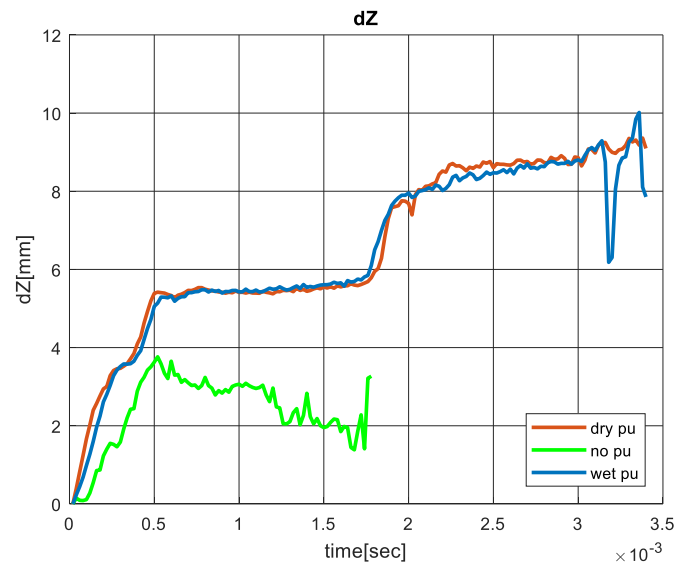


Fig. 7. Center point deflection history under 4 bar driving pressure.

Table 3

Ranking plate performance by. 1 corresponds to the minimal measured residual deflection while 2 and 3 include also possible early breaching of the plate.

Experiment set	Representative pressure peak	No polyurea	Dry polyurea	Wet polyurea
[1]	20 bar	3	2	1
3 bar	200 bar	3	2	1
3.5 bar	350 bar	3	1	2
4 bar	500 bar	3	1	2

wet side placement which can only affect at the early stages of the fluid structure interaction.

Finally, looking at results for a 4-bar pressure, a radically different picture emerges, as shown in Fig. 7.

The no polyurea plate signal is noisy and is only placed here as an illustration. The measured results should be viewed with care as the painted speckle pattern chipped off early in the deformation process while the plate itself failed shortly after.

Yet, both coated plates performed almost identically, with a small

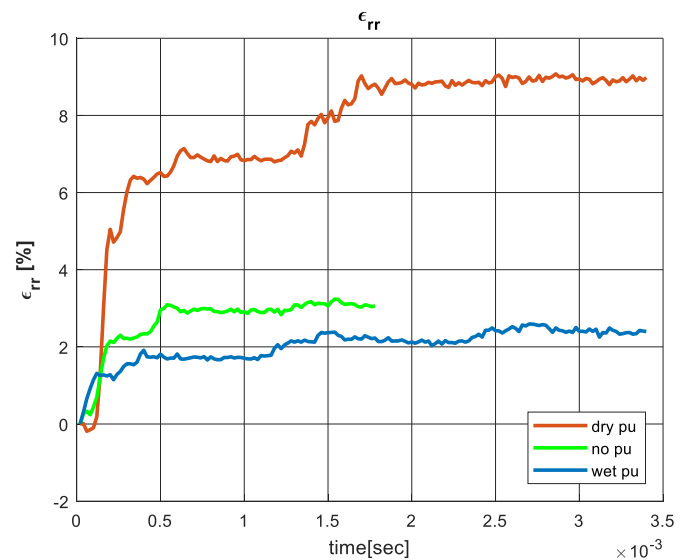


Fig. 8. Center point radial strain history under 3 bar driving pressure.

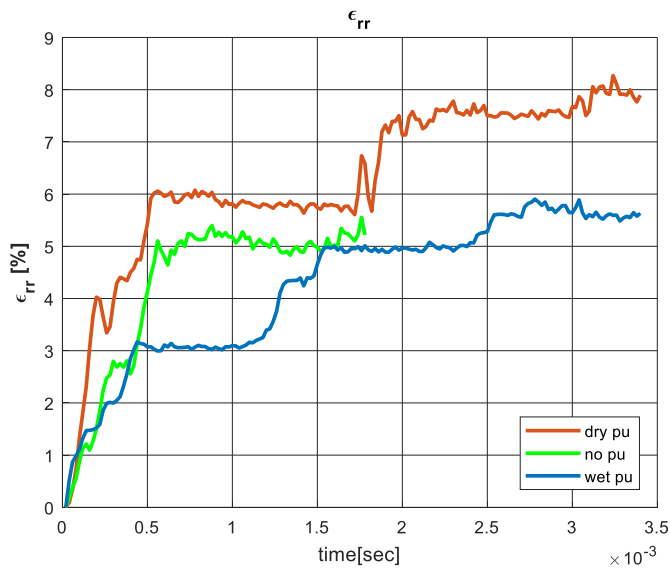


Fig. 9. Center point radial strain history under 3.5 bar driving pressure.

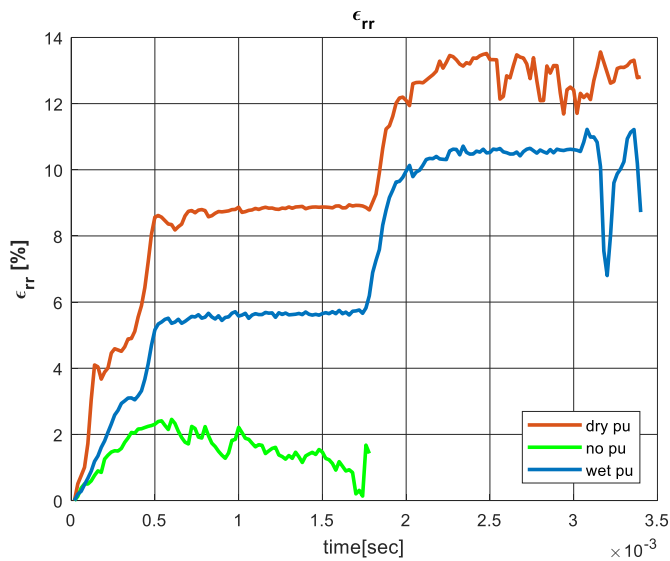


Fig. 10. -Center point radial strain history under 4 bar driving pressure.

difference at a later stage. This small difference is the initiation of failure in the wet polyurea plate which was breached this time. The only plate that survived the shock is the dry polyurea plate, as one can also see in Table 2 and in Fig. 12.

At this stage, one can rank the performance of the different layouts tested at different pressures, including our former results [1], as shown in Table 3. Note that the ranking is either based on best (1) corresponding to minimal residual deflection, (2 and 3) likewise, but also including early breaching.

From this table, one can notice that up to 200 bar, the wet polyurea clearly performs best whereas between 200 and 350 bar and beyond, the order of performance changes (reverts), favoring now placement of the polyurea on the dry side of the plate.

3.5. Center point strains

The center point strain's evolution is shown for the various applied pressures in Figs. 8–10.

One can see in Fig. 8 the relatively high strains which were measured on the dry polyurea plate center point compared to both other plates. This is another indication of the polyurea reinforcement concentrating the deflection at the center of the plate. This might be the result of water cavitation at the center of the plate as discussed earlier, but this remains to be further validated. Both the no polyurea and the wet polyurea plates perform similarly up to the point in which the no polyurea plate failed. The failure was not initiated at the center point which explains why both plates perform similarly at the center point but only one plate failed.

Fig. 9 shows the performance gaps between plates closing. As the shocks grow harder, the strain rate rises, which stiffens the polyurea [28]. The stiff polyurea is less effective in mitigating the fluid structure interaction, thus making the wet polyurea layer ineffective against the shock. We see that the no polyurea and the dry polyurea plates perform similarly up until the no polyurea plate failure, with the wet polyurea plate showing lower center point deflections.

In Fig. 10, the no polyurea plate center point strain is the lowest of all plates. This is misleading as the plate erupted very early in the experiment and its signal is shown here for reference only. The wet polyurea plate center point strain experiences a sudden drop nearing the end of the signal. This drop is probably due to the initiation of failure and the consequent loss of stability. The dry polyurea plate shows highest strains but even so, it is the only plate that survived the experiment as shown in Fig. 11. It is important to note here that the center point strain is not a good predictor of failure as the failure did not initiate at the center of the plate in any of the experiments.

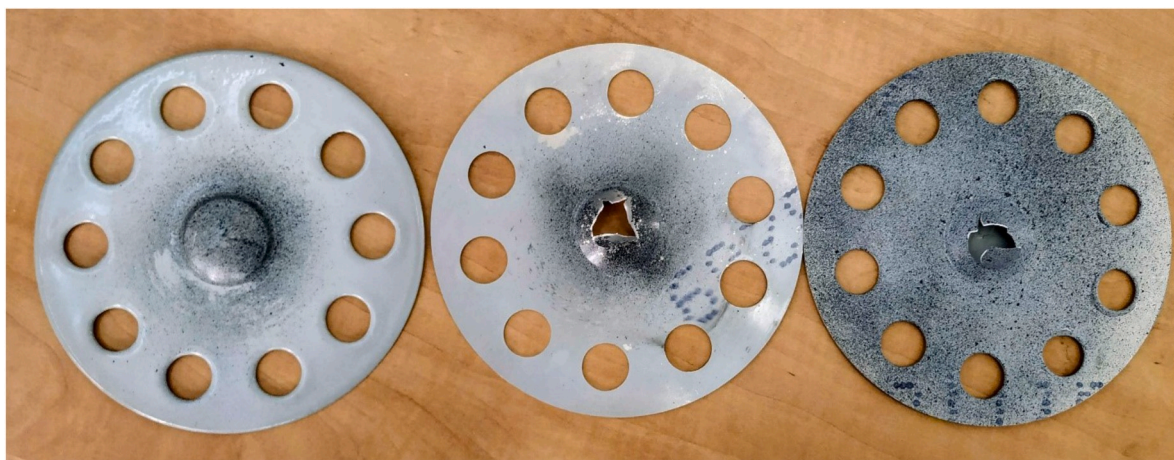


Fig. 11. Specimen plates after 4 bar experiments: left to right: dry polyurea, no polyurea, wet polyurea.

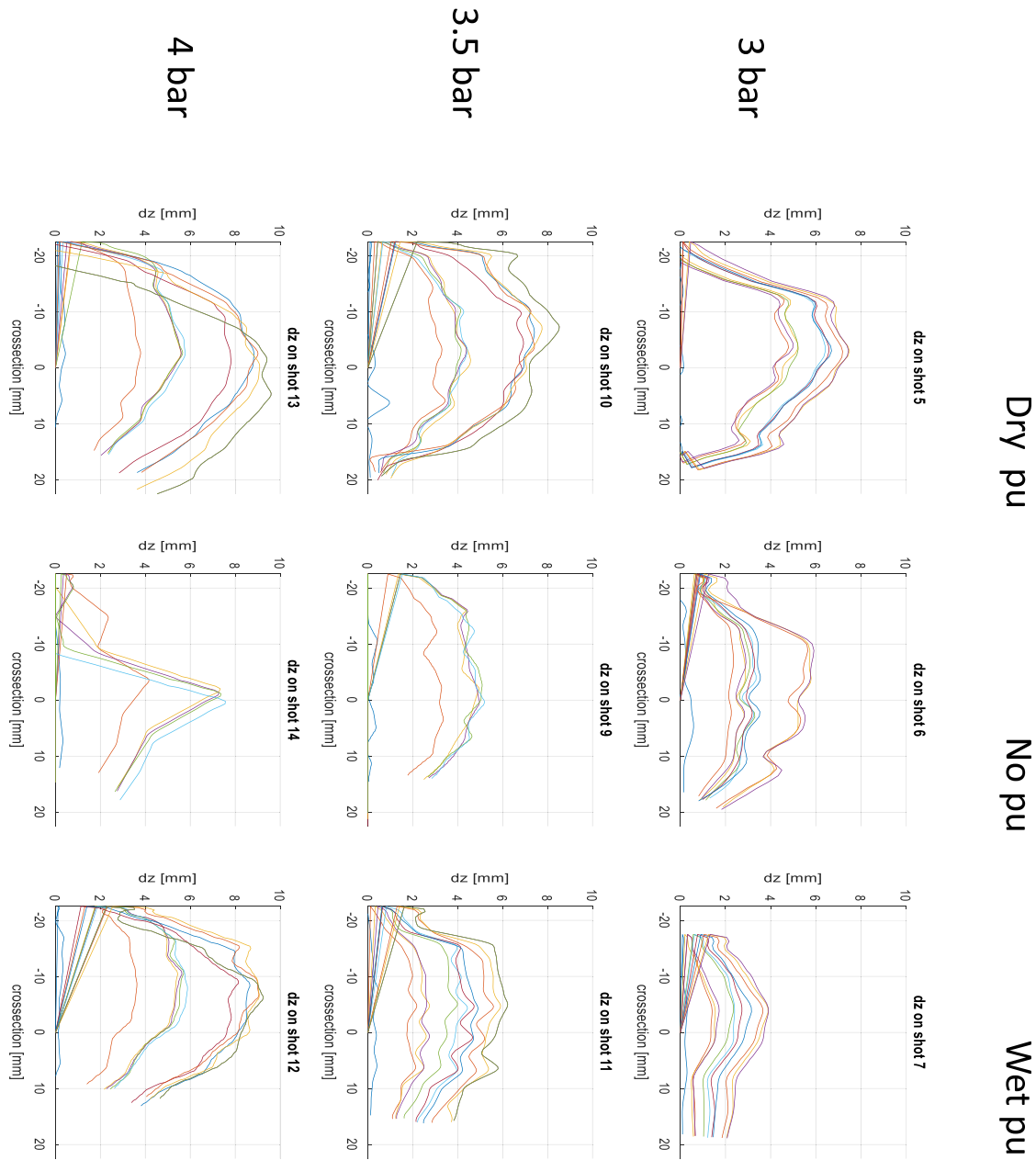


Fig. 12. Deflection histories of the specimen plates along a centerline.

3.6. Centerline deflection distribution history

Another significant result which we shall discuss is the evolution and distribution of deflection during the shock along the centerline of the plates. In the following plots, each line represents the profile of the plate at a certain moment during deformation, so each plot represents the full deformation history of a plate profile, as shown in Fig. 12.

One might notice that there are less lines in the no polyurea plates plots. This is due to early plate failures resulting in loss of DIC tracking ability. The speckle paint was severely chipped and was no longer analyzable due to the shocks. Yet, examining the deflection profiles, one can notice the following trends.

For the no polyurea specimen plates, the deflections are not distributed in an orderly fashion (vibrations are apparent in the signal). This is a sign of instability and indeed those plates failed early in the deformation process.

Next, when comparing the wet polyurea and the dry polyurea specimens loaded under 3 and 3.5 bar, the dry polyurea plate tends to form a dome shape while the wet polyurea deflections are more evenly distributed. This is an outcome of both the decreased momentum affecting the wet polyurea plate as well as the increased stiffness of the dry polyurea plate attributed to polyurea reinforcement, perhaps concomitant with cavitation in the water.

For the dry polyurea plates, deflections tend to accumulate in the center, leading to high strain at the center point whilst the wet polyurea plate naturally distributes the strains in a significant even fashion. The homogeneous distribution of strain along the cross section increases survivability in case of shock, hence, for relatively weak shocks, it seems better to apply polyurea on the wet side of the plate.

However, the 4 bar plot yields a totally different picture. The wet polyurea plate forms a dome just like the dry polyurea plate. It might be that the high rate sensitivity of polyurea has made it stiffer than the

aluminum base plate. In such a case, not only that hardened polyurea has a negligible damping effect, but it also increases the absorbed momentum as the overall structure is stiffer [33]. Since the polyurea is on the wet side, it cannot mitigate part of the shock experienced by the plate as the shocks in the polyurea layer are more intense than those in the next aluminum layer. In case of such a severe shock, it is apparently preferable to place the polyurea on the dry side, noting that the only plate which survived the 4 bar shock was the dry plate (Table 2 & Fig. 11).

4. Discussion and conclusions

Deflections and strains of polyurea coated aluminum plates were measured under hydrodynamic loading conditions using a single camera stereo DIC. We found that under mild shocks (up to 200 bar in this case) it is preferable to apply the coating to the side interacting with the water as the polyurea has a soothing effect on the interaction. When placed on the wet side of the plate, we suspect the polyurea can reduce the impulse acting on the plate as stiffer structures absorb more momentum during impact [33]. On the contrary, when the shocks are violent (200 bar and beyond), the polyurea layer experiences a severe compressive load, increasing its bulk modulus and disabling its FSI damping effect. Moreover, a polyurea coating applied to the dry side might absorb some momentum from the aluminum layer and mitigate it through one of the few mechanisms which give polyurea its shock mitigation capabilities [34, 35], for example, a glassy transition of the soft phase of polyurea or dispersion by the fiber like structure of the material. Let us note here that the previous results reported on the subject, and subsequent conclusions on the recommended placement of the polyurea layer, did not vary expressively with the shock amplitude as in the present work. The current results point of a transition that depends on the shock amplitude, tentatively identified to lie in the range of 200–350 bar without further precision.

To conclude, this work shows that there is no single “gold standard” to placing polyurea as a protective layer where a fluid carries the load to the structure (air explosion, hydrodynamic shocks etc.). The threat’s amplitude is a decisive factor when using polyurea as a protective layer, and the designer must account for this factor prior to selecting the side to be coated for optimal protection. However, the exact “transitional shock intensity” that reverses the trend for polyurea placement layer is yet to be identified.

This study complements the existing state of the art by emphasizing the anticipated shock intensity (and by that, the threat causing the shock) as determinant for the optimal protective layer placement.

Declaration of competing interest

The authors declare that they have no known competing financial interests or personal relationships that could have appeared to influence the work reported in this paper.

CRediT authorship contribution statement

O. Rijensky: Conceptualization, Methodology, Formal analysis, Investigation, Writing - original draft, Writing - review & editing, Visualization. **D. Rittel:** Writing - review & editing, Supervision, Funding acquisition.

Acknowledgement

The authors wish to acknowledge Mr. Benny Danino and Sela Industries for their kind technical assistance and supply of the experimental specimens.

References

- [1] O. Rijensky, D. Rittel, Polyurea coated aluminum plates under hydrodynamic loading: does side matter? *Int. J. Impact Eng.* 98 (2016) 1–12, <https://doi.org/10.1016/j.ijimpeng.2016.07.006>.
- [2] a.V. Amirkhizi, J. Isaacs, J. McGee, S. Nemat-Nasser, An experimentally-based viscoelastic constitutive model for polyurea, including pressure and temperature effects, *Philos. Mag. A* 86 (2006) 5847–5866, <https://doi.org/10.1080/14786430600833198>.
- [3] C.M. Roland, J.N. Twigg, Y. Vu, P.H. Mott, High strain rate mechanical behavior of polyurea, *Polymer* 48 (2007) 574–578, <https://doi.org/10.1016/j.polymer.2006.11.051>.
- [4] S.S. Sarva, S. Deschanel, M.C. Boyce, W. Chen, Stress–strain behavior of a polyurea and a polyurethane from low to high strain rates, *Polymer* 48 (2007) 2208–2213, <https://doi.org/10.1016/j.polymer.2007.02.058>.
- [5] J.A. Pathak, J.N. Twigg, K.E. Nugent, D.L. Ho, E.K. Lin, P.H. Mott, et al., Structure evolution in a polyurea segmented block copolymer because of mechanical deformation, *Macromolecules* 41 (2008) 7543–7548, <https://doi.org/10.1021/ma8011009>.
- [6] P.H. Mott, C.B. Giller, D. Fragiadakis, D.A. Rosenberg, C.M. Roland, Deformation of polyurea: where does the energy go? *Polymer* 105 (2016) 227–233, <https://doi.org/10.1016/j.polymer.2016.10.029>.
- [7] M. Grujicic, B. Pandurangan, T. He, B.A. Cheeseman, C.-F. Yen, C.L. Randow, Computational investigation of impact energy absorption capability of polyurea coatings via deformation-induced glass transition, *Mater. Sci. Eng., A* 527 (2010) 7741–7751, <https://doi.org/10.1016/j.msea.2010.08.042>.
- [8] W.G. Knauss, *Viscoelastic Material Characterization Relative to Constitutive and Failure Response of an Elastomer*, 2004.
- [9] M.L. Williams, R.F. Landel, J.D. Ferry, The temperature dependence of relaxation mechanisms in amorphous polymers and other glass-forming liquids, *J. Am. Chem. Soc.* 77 (1955) 3701–3707, <https://doi.org/10.1021/ja01619a008>.
- [10] J. Shim, D. Mohr, Rate dependent finite strain constitutive model of polyurea, *Int. J. Plast.* 27 (2011) 868–886, <https://doi.org/10.1016/j.ijplas.2010.10.001>.
- [11] C. Li, J. Lua, A hyper-viscoelastic constitutive model for polyurea, *Mater. Lett.* 63 (2009) 877–880, <https://doi.org/10.1016/j.matlet.2009.01.055>.
- [12] Y. Bai, C. Liu, G. Huang, W. Li, S. Feng, Y. Bai, et al., A hyper-viscoelastic constitutive model for polyurea under uniaxial compressive loading, *Polymers* 8 (2016) 133, <https://doi.org/10.3390/polym8040133>.
- [13] R.W. Ogden, Large deformation isotropic elasticity - on the correlation of theory and experiment for incompressible rubberlike solids, *Proc R Soc A Math Phys Eng Sci* 326 (1972) 565–584, <https://doi.org/10.1098/rspa.1972.0026>.
- [14] B. Bernstein, E.A. Kearsley, L.J. Zapas, A study of stress relaxation with finite strain, *Rubber Chem. Technol.* 38 (1965) 76–89, <https://doi.org/10.5254/1.3535640>.
- [15] Y.A. Bahei-El-Din, G.J. Dvorak, Behavior of sandwich plates reinforced with polyurethane/polyurea interlayers under blast loads, *J. Sandw. Struct. Mater.* 9 (2007) 261–281, <https://doi.org/10.1177/1099636207066313>.
- [16] Y.A. Bahei-El-Din, G.J. Dvorak, O.J. Fredricksen, A blast-tolerant sandwich plate design with a polyurea interlayer, *Int. J. Solid Struct.* 43 (2006) 7644–7658, <https://doi.org/10.1016/j.ijlsolstr.2006.03.021>.
- [17] M.R. Amini, J. Simon, S. Nemat-Nasser, Numerical modeling of effect of polyurea on response of steel plates to impulsive loads in direct pressure-pulse experiments, *Mech. Mater.* 42 (2010) 615–627, <https://doi.org/10.1016/j.mechmat.2009.09.009>.
- [18] S.A. Tekalur, A. Shukla, K. Shivakumar, Blast resistance of polyurea based layered composite materials, *Compos. Struct.* 84 (2008) 271–281, <https://doi.org/10.1016/j.compstruct.2007.08.008>.
- [19] K. Ackland, C. Anderson, T.D. Ngo, Deformation of polyurea-coated steel plates under localised blast loading, *Int. J. Impact Eng.* 51 (2013) 13–22, <https://doi.org/10.1016/j.ijimpeng.2012.08.005>.
- [20] S.N. Raman, T. Ngo, P. Mendis, T. Pham, Elastomeric polymers for retrofitting of reinforced concrete structures against the explosive effects of blast, *Ann. Mater. Sci. Eng.* 2012 (2012) 1–8, <https://doi.org/10.1155/2012/754142>.
- [21] L. Xue, W. Mock, T. Belytschko, Penetration of DH-36 steel plates with and without polyurea coating, *Mech. Mater.* 42 (2010) 981–1003, <https://doi.org/10.1016/j.mechmat.2010.08.004>.
- [22] T. El Sayed, W. Mock, A. Mota, F. Fraternali, M. Ortiz, Computational assessment of ballistic impact on a high strength structural steel/polyurea composite plate, *Comput. Mech.* 43 (2008) 525–534, <https://doi.org/10.1007/s00466-008-0327-6>.
- [23] D. Mohotti, T. Ngo, P. Mendis, S.N. Raman, Polyurea coated composite aluminium plates subjected to high velocity projectile impact, *Mater. Des.* 52 (2013) 1–16, <https://doi.org/10.1016/j.matdes.2013.05.060>.
- [24] M. Grujicic, W.C. Bell, B. Pandurangan, T. He, Blast-wave impact-mitigation capability of polyurea when used as helmet suspension-pad material, *Mater. Des.* 31 (2010) 4050–4065, <https://doi.org/10.1016/j.matdes.2010.05.002>.
- [25] C.M. Roland, D. Fragiadakis, R.M. Gamache, Elastomer–steel laminate armor, *Compos. Struct.* 92 (2010) 1059–1064, <https://doi.org/10.1016/j.compstruct.2009.09.057>.
- [26] J. LeBlanc, N. Gardner, A. Shukla, Effect of polyurea coatings on the response of curved E-Glass/Vinyl ester composite panels to underwater explosive loading, *Compos. B Eng.* 44 (2013) 565–574, <https://doi.org/10.1016/j.compositesb.2012.02.038>.
- [27] J. LeBlanc, C. Shillings, E. Gauch, F. Livolsi, A. Shukla, Near field underwater explosion response of polyurea coated composite plates, *Exp. Mech.* (2015), <https://doi.org/10.1007/s11340-015-0071-8>.

- [28] M.R. Amini, J. Isaacs, S. Nemat-Nasser, Investigation of effect of polyurea on response of steel plates to impulsive loads in direct pressure-pulse experiments, *Mech. Mater.* 42 (2010) 628–639, <https://doi.org/10.1016/j.mechmat.2009.09.008>.
- [29] H.D. Espinosa, S. Lee, N. Moldovan, A novel fluid structure interaction experiment to investigate deformation of structural elements subjected to impulsive loading, *Exp. Mech.* 46 (2006) 805–824, <https://doi.org/10.1007/s11340-006-0296-7>.
- [30] V.S. Deshpande, A. Heaver, N.A. Fleck, An underwater shock simulator, *Proc R Soc A Math Phys Eng Sci* 462 (2006) 1021–1041, <https://doi.org/10.1098/rspa.2005.1604>.
- [31] J.F. Cardenas-Garcia, H.G. Yao, S. Zheng, 3D reconstruction of objects using stereo imaging, *Optic Laser. Eng.* 22 (1995) 193–213, [https://doi.org/10.1016/0143-8166\(94\)00046-D](https://doi.org/10.1016/0143-8166(94)00046-D).
- [32] M. Sutton, W. Wolters, W. Peters, W. Ranson, S. McNeill, Determination of displacements using an improved digital correlation method, *Image Vis Comput.* 1 (1983) 133–139, [https://doi.org/10.1016/0262-8856\(83\)90064-1](https://doi.org/10.1016/0262-8856(83)90064-1).
- [33] G. Taylor, The pressure and impulse of submarine explosion waves on plates - the scientific papers of G.I. Taylor, 1963 Cited by 291 Related articles, *Sci Pap GI Taylor* 3 (1941) 287–303.
- [34] M. Grujicic, B. Pandurangan, T. He, B.A. Cheeseman, C.-F. Yen, C.L. Randow, Computational investigation of impact energy absorption capability of polyurea coatings via deformation-induced glass transition, *Mater. Sci. Eng., A* 527 (2010) 7741–7751, <https://doi.org/10.1016/j.msea.2010.08.042>.
- [35] M. Grujicic, B. Pandurangan, W.C. Bell, B.A. Cheeseman, C.-F. Yen, C.L. Randow, Molecular-level simulations of shock generation and propagation in polyurea, *Mater. Sci. Eng., A* 528 (2011) 3799–3808, <https://doi.org/10.1016/j.msea.2011.01.081>.